Smart Structures and Systems, *Vol. 27, No. 4 (2021) 651-666*
DOI: https://doi.org/10.12989/sss.2021.27.4.651

Hybrid-ANFIS approaches for compressive strength prediction of cementitious mortar and paste employing magnetic water

Mosbeh R. Kaloop [1,2,3a], Omar M.M. Yousry [4b], Pijush Samui [5c], Mohamed M.Y. Elshikh [6d] and Jong Wan Hu*[1,2]

[1] *Department of Civil and Environmental Engineering, Incheon National University, Korea*
[2] *Incheon Disaster Prevention Research Center, Incheon National University, Korea*
[3] *Public Works and Civil Engineering Department, Mansoura University, Egypt*
[4] *Structural Engineering Department, Tanta University, Egypt*
[5] *Department of Civil Engineering, National Institute of Technology Patna, India*
[6] *Structural Engineering Department, Mansoura University, Egypt*

(*Received June 7, 2020, Revised December 3, 2020, Accepted December 19, 2020*)

Abstract. The compressive strength is an important mechanical feature of concrete that is needed in construction design. Thus, a lot of investigations were carried out to predict the compressive strength of various concretes. However, the prediction models for the compressive strength of cement mortar or paste that include magnetic water (MW) and granulated blast-furnace slag (GBFS) are still limited. The current study has developed hybrid algorithms based on adaptive neuro-fuzzy inference system (ANFIS) for modeling the compressive strength of cement mortar and paste that made with MW and GBFS as a novel mixture content. A total of 144 experimental sets of concrete-compressive strength tests for each cement mortar and paste were collected to train and validate the proposed methods, in which the cycles number of water magnetization, cement, GBFS, superplasticizer contents and curing time are set as the input data while the compressive strength value is set as the output. The developed hybrid algorithms of ANFIS optimized by firefly algorithm (FA), Improved Particle Swarm Optimization (IPSO) and biogeography-based optimization (BBO) algorithms for predicting the compressive strength of the mortar and paste. The proposed models and relevance vector machine (RVM) approach were evaluated and compared. The results showed that the ANFIS-FA outperforms other models for modeling the compressive strength of cement mortar and paste. The adjusted-coefficient of determination and root mean square error values of cement mortar models (96.20%, 92.33%, 92.36% and 89.41%) and (2.17 MPa, 3.10 MPa, 3.18 MPa and 3.06 MPa) and of cement paste models (96.92%, 80.91%, 92.19% and 88.18%) and (2.45 MPa, 5.80 MPa, 4.39 MPa and 5.20 MPa) were determined for ANFIS-FA, ANFIS-IPSO, ANFIS-BBO and RVM models, respectively, which indicate that the ANFIS-FA is a suitable model for estimating the compressive strength of cement mortar and paste that include MW. Moreover, the sensitivity of MW and GBFS is shown high for modeling the compressive strength of cement mortar.

Keywords: cement mortar and paste; magnetic water; ANFIS; hybrid model

1. Introduction

Over the decades, the quality of concrete and cement productions are essentially required for civil engineering applications, including the construction requirements (Chu 2019, Torres and Seo 2017). The key hardened property of cement mortar and paste quality is the compressive strength (CS) of them (Chu 2019, Dhir *et al*. 2017, Taylor *et al*. 2012). The cement mortar and paste are considered to be a composite material consisting of a mixture of cement with and without fine aggregate, for the mortar and paste, respectively, and water amount for the hydration process (Chu 2019, Yousry *et al*. 2020). Fine and coarse aggregates were found to significantly affect the concrete characteristics (Torres and Seo 2017, Torres *et al*. 2017, Seo and Pokhrel 2019). Recently, mineral additives, such as fly ash, lime, granulated blast-furnace slag (GBFS), palm oil fuel ash and silica have been widely added for producing of cement mortar and paste (Ma *et al*. 2019, Qadir *et al*. 2019; Safiuddin *et al*. 2016, Yousry *et al*. 2020). These additives decrease using Portland cement and improving the characteristics of cement productions (Ma *et al*. 2019, Yousry *et al*. 2020). Ma *et al*. (2019) showed that the addition of slag improved the physical and mechanical properties of mortars. Kockal *et al*. (2017, 2018) found the mechanical characteristics of concrete is improved by adding slag in the mixture of concrete with applying milling process of it. The compressive strength and workability of cement mortar were improved by adding lime (Qadir *et al*. 2019). Also, mineral additives affect the thermal condition of the concrete (Kockal 2015).

Meanwhile, magnetic water (MW) affects the performance of hardened and fresh characteristics of

*Corresponding author, Associate Professor,
E-mail: jongp24@inu.ac.kr
[a] Associate Professor
[b] Master Student
[c] Professor
[d] Prfessor

ISSN: 1738-1584 (Print), 1738-1991 (Online)

cement mortar and paste (Khorshidi *et al*. 2014, Yousry *et al*. 2020). For instance, Khorshidi *et al*. (2014) concluded that the MW improved the CS and workability of cement paste by 10%. Yousry *et al*. (2020) found that the CS of cement mortar can be increased up to 60% by using 150 - cycle MW in mortar mixtures. Furthermore, MW increased the CS of self-compacting concrete (Esfahani *et al*. 2018). Moreover, MW influenced the admixture contents by decreasing the water content of the concrete and reducing superplasticizer dosage of the mortar or paste (Esfahani *et al*. 2018, Khorshidi *et al*. 2014, Yousry *et al*. 2020). More details for the effects of MW on the cement mortar/paste and concrete properties and admixture contents can be found in (Bharath *et al*. 2016, Su *et al*. 2000, Wang *et al*. 2018). The current study uses MW and GBFS as a novel additive content for producing cement mortar and paste. The CS of cement mortar and paste was determined at the age of 28 days.

The conventional methods for estimating CS of cement mortar or paste, including mechanical tests and preparation of large numbers of specimens, are time-consuming and costly. In recent years, soft computing techniques have been widely and successfully used to estimate the CS of concrete or cement mortar and paste. For example, the Relevance Vector Machine (RVM) was shown to be robust for estimating the CS of concrete that included silica fume contents (Biswas *et al*. 2019). Also, the RVM was used to estimate the CS of concrete, including GBFS additive contents, and the results showed its performance was an agreement with experimental results (Prasanna *et al*. 2018). In addition, the RVM outperformed than least square support vector machine (LSSVM) for estimating the CS of self-compacting concrete (Aiyer *et al*. 2014). Furthermore, the performance of RVM was shown to be acceptable for predicting the CS of cement mortar (Mishra *et al*. 2019b, Verma *et al*. 2017) and other concrete characteristics (Yuvaraj *et al*. 2014). Artificial neural network (ANN) was successfully applied to predict the CS of concrete (Seo *et al*. 2015, 2017, Al-Swaidani and Khwies 2018). In the same time, the fuzzy logic was found more explicit and useful than the ANN for predicting the CS of cement mortar (Akkurt *et al*. 2004), and concrete (Aggarwal *et al*. 2013, Tayfur *et al*. 2014). Recently, adaptive neuro-fuzzy inference system (ANFIS) significantly applied to predict different concrete performances; while, it possesses advantages of both fuzzy logic and ANN (Prasad Meesaraganda *et al*. 2020). Sinha *et al*. (2019) applied the ANFIS for predicting the early age of CS of high-performance concrete, and their results showed it could be considered as one of the best reliable tools for modeling the relationship between inputs and output variables. In addition, the ANFIS model outperforms statistical models for predicting CS of lightweight concrete (Razavi Tosee and Nikoo 2019). The CS of brick-mortar masonry structures was also estimated using ANFIS, and the results showed its performance high for modeling the CS (Mishra *et al*. 2019a). Also, ANFIS was applied to predict the weight loss of cement (Boukhari 2020), the strength of rubber concrete (Jalal *et al*. 2020) and characteristics of concrete (Mansouri *et al*. 2016, 2017, 2018, 2019). More recently, hybrid ANFIS algorithms have been developed to map a nonlinearity relationship between inputs and outputs variables of different concrete performances. Ly *et al*. (2019) improved the performance of the ANFIS model for estimating CS of concrete by optimizing it using Principal Component Analysis (PCA) together with Teaching-Learning-Based Optimization (TLBO) methods. Furthermore, a combination of ANFIS with Gases Brownian Motion Optimization (GBMO) was proposed and evaluated for estimating the CS of high-performance concrete, and the proposed model performance was acceptable to estimate the CS in limited reiterations (Rahchamani *et al*. 2019). Herein, many algorithms can be used to improve ANFIS performance in the modeling algorithms; among these are firefly algorithm (FA) (Kamarian *et al*. 2014, Moghadam *et al*. 2019, Riahi-Madvar *et al*. 2020), Improved Particle Swarm Optimization (IPSO) (Rayen and Subhashini 2019, Selma *et al*. 2020, Xiao *et al*. 2014) and biogeography-based optimization (BBO) (Ahmadlou *et al*. 2019, Jaafari *et al*. 2019, Termeh *et al*. 2019) algorithms. The performance of integration ANFIS with FA, IPSO and BBO showed great potential by considering the model accuracy and computational time (Ahmadlou *et al*. 2019, Moghadam *et al*. 2019, Selma *et al*. 2020).

Based on our state-of-the-art, it can be seen that hybrid models have shown good performance in different prediction applications. However, the prediction models for CS of cement mortar or paste that include MW and GBFS are still limited. Therefore, this study investigates to develop novel hybrid algorithms of ANFIS optimized by FA, IPSO and BBO methods for predicting the CS of the mortar and paste includes MW and GBFS. The results of the proposed hybrid ANFIS approaches and conventional ANFIS model were compared to the RVM model, in which hyperparameters were determined using the trial-and-error method. The models were evaluated based on different error indices and residual analysis. The training and testing datasets of the proposed models were experimentally implemented utilizing different additives contents of GBFS and magnetization cycles for producing MW.

2. Material and methods

2.1 Materials used and experimental mixture design

2.1.1 Materials descriptions

Cement: CEM I class (42.5 N) of the chemical composition shown in Table 1A was used in this study, which was purchased from a local store (Suez Cement Company). Cement conforms to ASTM C150 Type1 (American Society for Testing and Materials International 2011) with a specific weight of 3.15. Physical and mechanical characteristics are calculated and recorded in Table 1B.

Sand: Siliceous natural sand compliant with ASTM C33(ASTM Standard C33, 2003) has been used. The sand was collected from a nearby warehouse. The physical

Table 1A Chemical composition of used cement (American Society for Testing and Materials International 2011)

Element	SiO_2	Al_2O_3	Fe_2O_3	CaO	MgO	Na_2O	SO_3	K_2O	LOI
Mass (%)	21.3	4.6	3.58	63.1	2.41	0.36	2.82	0.22	2.15
ASTM C150 Limit	-	-	-	-	≤ 6	-	≤ 3.5	-	-
Bouge composition	C3S	C2S	C3A	C4AF					
Mass (%)	46	26	6	11					
Limit	-	-	-	-					

Table 1B Physical and mechanical properties of used cement

Element	Blain fineness (cm^2/g)	Initial setting time (min)	Final setting time (min)
Value	3000	180	300
Condition	-	Tap water	Tap water

Table 1C Physical properties of used sand

Element	Fineness modulus	Specific gravity	Bulk density (Kg/m^3)	Moisture content (%)	Volume increase (%)	Water absorption (%)
Value	3.31	2.672	1573.61	1.56	0.919	0.818

properties of the fine aggregate are shown in Table 1C, while the sieve analysis is shown in Fig. 1(a).

Superplasticizer: Sikament 163 superplasticizer (Type F) with a specific gravity of 1.1 was developed by SIKA CO.

Granulated blast-furnace slag (GBFS): GBFS is procured from corporation ELMOTAHIDA, Cairo, Egypt. Its physical and chemical characteristics are shown in Table 2. In this study, GBFS is used in the mixing process to replace cement.

Table 2 Physical and chemical properties of GBFS

Test item	Test result	Reference standard
Physical properties		
Fineness (cm^2/g)	421.2	> 330
After #325 sieving	9.5	< 20
Sp. gr	2.94	-
Chemical properties		
Air content of paste (%)	3.56	< 12
Activity, 3 days (%)	75.1	-
Loss of ignition (%)	0.441	-
SiO_2 (%)	34.56	-
Al_2O_3 (%)	13.21	-
Fe_2O_3 (%)	0.314	-
CaO (%)	40.32	-
MgO (%)	7.46	< 4
SO_3 (%)	1.25	> 1.4
Alkalinity	1.55	< 2.5
Sulfide sulfur	0.57	-
K_2O (%)	0.281	-
Na_2O (%)	0.083	-

Water: Two types of water have been used; tap water (TW) and MW. The MW was produced by passing water through a magnetizer with a magnetic intensity of 1.4 Tesla. The magnetizer was produced by the Delta Water Company, Alexandria, Governorate of Alexandria, Egypt. It was installed at the lab through some preparations for the creation of a circulation device. This device passed the water in a cyclical manner. The surface tension of the water was determined and found to be 0.06624 N/m, which demonstrated a substantial improvement and prepared the water for the next level. As seen in Fig. 1(b), the system consists of the following: the water supply (1), the bucket that holds the water to be magnetized, the pump (2), which drags the water from the container bucket and then moves it through the pipes (3), the calibration valve (4), the 1.5" valve used to brace the pump for dragging water, the water protection valve (5), the control valve used not to render the

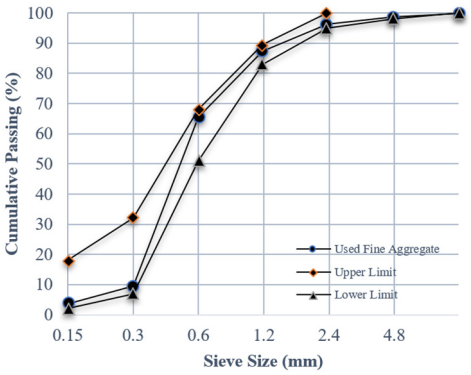

(a)

(b)

Fig. 1 (a) Particle size distribution (Sieve Analysis) for used fine aggregate; and (b) Water Magnetization Process

flow. The magnetizer (6), the instrument itself, which carried out a magnetization test on the surface. Next, the length of the process is determined, the pump continues drawing water up from the water supply to move it through the magnetizer, and then returns to another container, i.e., water has completed one cycle. The time needed for a single cycle was 36 s. According to Eq. (1), the water discharge rate is measured and estimated to be 9 lit/min, and then regulated using the safety valve for all mixtures.

$$\text{Water discharge Rate (Q)} = \frac{\text{Volume (lit)}}{\text{time (min)}} \quad (1)$$

In order to get further cycles, the time needed for the desired number of cycles is determined by equation (2), so the system runs for the specified time, indicating that the water outlet is returned to the water supply again, i.e., closed circulation, as seen in Fig. 1(b).

$$\text{Targeted Cycles Time (min)} = \text{Number of cycles} \times \frac{\text{one cycle time (sec)}}{60\ (\text{sec/min})} \quad (2)$$

2.1.2 Mixing proportions

The testing system concluded with 72 combinations. The mixtures were split into two main groups. The first section consists of 36 mixtures of cement mortar, while the second one includes 36 mixtures of cement paste. The two divisions were divided into four classes, each comprising nine mixtures. The water used was the TW in the first group however the water used in the 2nd, 3rd and 4th classes were MW, which varied from each other in the number of cycles of 50 cycles, 100 cycles and 150 cycles, respectively while exploring the impact of the time spent in magnetizing water. Each of the eight groups was classified into three subgroups.

The 1st subgroup was treated without any superplasticizer, whilst the 2nd and 3rd subgroups were provided with 0.5 percent, and 1 percent of the superplasticizer by weight of binders, respectively. Subgroups have been developed to analyze the dosage of the superplasticizer. The three mixtures in each subgroup are distinct from each other to analyze the effect of increasing the dosage of GBFS (0,10 per cent and 20 per cent by weight of binders). The amounts of mixtures of cement mortar and cement paste are listed in Appendices A1 and A2, respectively.

To produce mixtures of paste and mortar, the ingredients to be blended are prepared, weighted, and packed for mixing. When using tap water, the superplasticizer was first applied to the water, but when using MW, it was placed into the bucket and then magnetized in the manner described above, then the superplasticizer was applied. The valve was used to control the flow rate of the water at 9 lit/min. Materials were initially combined in a dry state using a hydraulic mixer to ensure homogeneity, and then the water, including a superplasticizer, was applied to the mixture. The average time of each mixture was 4-5 minutes.

Wooden shapes, including separators, to form 70 mm × 70 mm × 70 mm cubes for cement mortar were used for compressive strength testing; however, similar shapes have been used for cement paste sizes of 50 mm × 50 mm × 50 mm. Since being destroyed at one day of maturity, all specimens (648 cubes) were cured in TW at 25°C for 3, 7 and 28 days. In both studies, triplicate specimens were used for each sample case, and the mean findings were then considered.

2.2 Models design

This study designs and evaluates a developed soft computing technique to estimate CS of cement mortar and paste that made with MW and GBFS as a novel mixture content. MATLAB software was used to design the proposed models. following is a summary of these models.

2.2.1 Relevance vector machine (RVM)

The RVM is a developed algorithm based on the support vector machine, that can be used for probabilistic classification and regression (Tipping 2000). The full description and mechanism of RVM for modeling can be found in (Prasanna *et al*. 2018, Yuvaraj *et al*. 2014). The sparse representation in RVM is attained by assuming a sparse distribution based on the weights of the input variables in the regression model (Verma *et al*. 2017). The low computational cost of RVM is the main advantage of this model (Verma *et al*. 2017). The map between inputs and output for RVM model can be expressed as follows

$$y(x) = \sum_{n=1}^{N} w_n K(x, x_n) + w_0 \quad (3)$$

where, N = data number; w_n are the model weights; w_0 is bias, and $K(x, x_n)$denotes a kernel function. Where, x is the input variables.

As presented in Eq. (3); it can be shown that the main factor in RVM for modeling is the Kernel function width which can be determined using post modeling analysis (Murthy *et al*. 2019, Tipping 2000). Post-modeling analysis in training and testing phases is associated with the number of relevance vectors (NRV) involved in the model and their corresponding weights and variations in kernel width (σ). Fig. 2(a) shows the RVM processing for the modeling CS of cement mortar and paste. In this study, the radial basis kernel (RBK) function, Eq. (4), was selected.

$$K(x, x_i) = exp\left(\frac{-(x - x_i)(x - x_i)^T}{2\sigma^2}\right) \quad (4)$$

Here, the σ was initially assumed as 0.13, and the optimum σ was 1 for the CS estimating of cement mortar and paste in the training phase. The coefficient of correlation (R) was used to assess the model performance in the design stage. A sparse solution was conducted. Herein, the following RVM models were obtained for the CS of cement mortar (Eq. (5)) and paste (Eq. (6)). Fig. 2(b) illustrates the CS model's weights for the cement mortar and paste.

$$CS_m = \sum_{i=1}^{101} w_i\, exp\frac{-(x - x_i)(x - x_i)^T}{2} \quad (5)$$

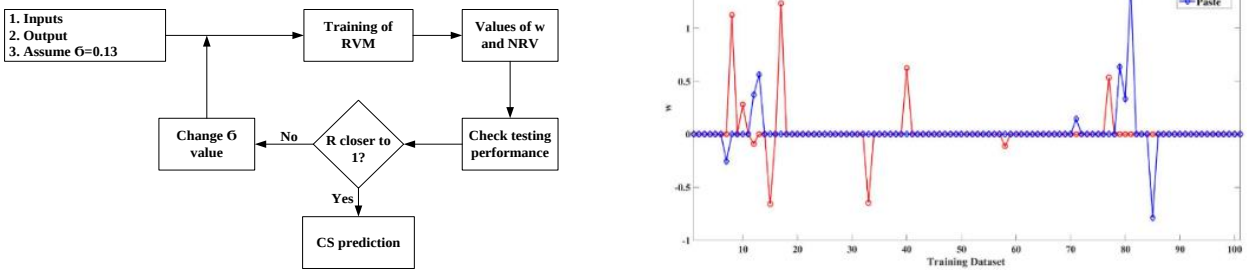

(a) (b)

Fig. 2 (a) RVM development model for CS prediction; (b) Values of weight vector for the developed RVM models

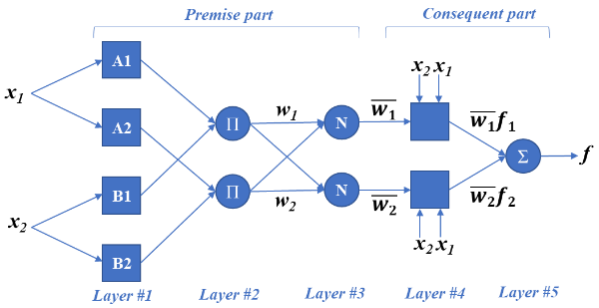

Fig. 3 The ANFIS diagram (Eldessouki and Hassan 2015)

$$CS_p = \sum_{i=1}^{101} w_i \, exp \frac{-(x - x_i)(x - x_i)^T}{2} \quad (6)$$

2.2.2 Adaptive neuro-fuzzy inference system (ANFIS)

The ANFIS is an integration algorithm that comprises ANN and fuzzy logic (FL) methods (Ly *et al*. 2019). Fig. 3 illustrates the ANFIS diagram for two inputs x_1 and x_2, as an example for the ANFIS processing. The ANFIS structure includes five layers, as presented in Fig. 3, which contains two adaptive layers (fuzzification and defuzzification) and three fixed layers (rule, normalization and aggregation) (Eldessouki and Hassan 2015, Jaafari *et al*. 2019, Ly *et al*. 2019, Termeh *et al*. 2019, Xiao *et al*. 2014). The adaptive layers are distributed between the premise and consequent parts; this allows these layers to adjust the performance of the ANFIS model (Eldessouki and Hassan 2015).

Commonly, the Takagi-Sugeno (TS) if-then rules and suitable membership function are used in ANFIS for fuzzy inference system; this provides the ANFIS to distinguish the nonlinearity relationship between inputs and output variables (Ly *et al*. 2019).

The rules of TS for two inputs x_1 and x_2 were expresses as:

Rule 1: if x_1 is A_1 and x_2 is B_1, then

$$f_1 = p_1 x_1 + q_1 x_2 + r_1$$

Rule 2: if x_1 is A_2 and x_2 is B_2, then

$$f_2 = p_2 x_1 + q_2 x_2 + r_2$$

Where, $A_{1,2}$ and $B_{1,2}$ are the fuzzy sets for inputs x_1 and x_2, respectively. $p_{1,2}$; $q_{1,2}$ and $r_{1,2}$ are the parameters of output function for the two rules calculated through the training process, and these parameters are used to improve the consequent part (Eldessouki and Hassan 2015).

Here, the summary of outputs of the five layers of the ANFIS model can be presented as follows

$$O_i^1 = \begin{cases} \mu_{A_i}(x_1) \\ \mu_{B_i}(x_2) \end{cases} \quad (7)$$

$$O_i^2 = w_i = \mu_{A_i}(x_1) \cdot \mu_{B_i}(x_2) \quad (8)$$

$$O_i^3 = \overline{w_i} = \frac{w_i}{\sum_{j=1}^{N} w_j} \quad (9)$$

$$O_i^4 = \overline{w_i} f_i = \overline{w_i}(p_i x_1 + q_i x_2 + r_i) \quad (10)$$

$$O_i^5 = f = \sum_{i=1}^{N} \overline{w_i} f_i \quad (11)$$

where, O represents the output of each calculation in the layers; μ_{A_i} and μ_{B_i} are the membership functions (MF) for x_1 and x_2 inputs, respectively; N is the number of inputs. The weight (or firing strength) and normalized matrices (w and $\overline{w}$, respectively) are calculated in the second and third layers, respectively.

In this study, the selected MF is the Gaussian (bell-shape) function with normalized output in between [0 and 1], which can be expressed for the input x1 as follows

$$\mu_{A_i}(x_1) = e^{-\left(\frac{x_1 - a_i}{b_i}\right)^2} \quad (12)$$

where, a and b are the parameters of MF. These parameters are used to improve the premise part (Eldessouki and Hassan 2015). Here, the hybrid learning algorithm presented in Eldessouki and Hassan (2015) was applied in this study to estimate the ANFIS parameters. The number and type MF are determined in the design stage. Here, ANFIS has three different FIS, that are grid partitioning (GP), subtractive clustering (SC) and fuzzy c-means (FCM) (Moghadam *et al*. 2019, Benmouiza and Cheknane 2019). In this study, the AFNIS with FCM gives the best performance in terms of RMSE. Also, 2 to 8 MF's are evaluated, and the results showed that with increasing the MF numbers, the accuracy of ANFIS is increased. In this study, 4 MF's were selected, since the changes of Akaike

information criterion (AIC) of the model that has MFs greater than 4 are insufficient.

Although the ANFIS performance was shown better than ANN and FL for nonlinear modeling of different concrete characteristics, it is still limited in calculating the accurate firing strength or weight matrix (Jaafari *et al*. 2019, Riahi-Madvar *et al*. 2020, Termeh *et al*. 2019). Many researchers had applied different optimization methods for improving the strength parameters, such as Genetic Algorithm (Hesami *et al*. 2019), PSO (Pannu *et al*. 2018), Grey Wolf optimizer (Jaafari *et al*. 2019), teaching-learning based optimization (Ly *et al*. 2019). The current study investigates the use of IPSO, FA, and BBO techniques to improve the ANFIS performance for estimating CS of cement mortar and paste.

2.2.3 Improved Particle Swarm Optimization (IPSO)

IPSO is an optimization algorithm that is currently applied to overcome the drawback of PSO technique, in fail to converge to the best position (Rayen and Subhashini 2019, Selma *et al*. 2020, Xiao *et al*. 2014). The D-dimensional space uses to fix the size agents in the PSO algorithm technique. The position and speed particles applied to a setting of the fuzzy logic controller and a modifying of parameters of the model between two simulations, respectively. The PSO started with generating a random swarm of particles for each parameter of the model. Next, the swarm was updated based on the position update of particles. The updated circulated up to obtain the optimum position of particles. The position update can be expressed as follows (Selma *et al*. 2020)

$$v_i^{t+1} = wv_i^t + c_1 r_1\left(p_{best,i}^t - X_i^t\right) + c_2 r_2\left(g_{best,i}^t - X_i^t\right) \quad (13)$$

$$X_i^{t+1} = X_i^t + v_i^{t+1} \quad (14)$$

where, X and v denote the position and speed of the particle, respectively; w is the inertia parameter; c_1 and c_2 represent the cognitive and social component parameters, respectively. r_1 and r_2 are randomly assumed in between 0 and 1. $p_{best,i}^t$ and $g_{best,i}^t$ are the best positions of the particle at individual and global positions, respectively.

In IPSO, a dynamic acceleration parameters adjustment is applied to estimate the cognitive and social component parameters. Moreover, an adaptive nonlinear adjustment weight is applied depending on the particle's fitness value. Furthermore, to improve the best performance of the particle's positions, the adaptive genetic operators (crossover operation and mutation operation) are employed. The detail of PSO and IPSO can be found in Rayen and Subhashini (2019). The pseudo-code that used in this study for CS of cement mortar and paste is presented in Algorithm 1.

In the current study, the parameters of IPSO were defined as follows for the CS estimation of cement mortar and paste: the size of particle swarm is 30, the maximum iteration is 1000, the initial random range of particles position and velocity are -1.0 to 1.0 and -0.5 to 0.5, respectively; $c_1 = c_2 = 0.30$. Herein, in the ANFIS-IPSO, IPSO utilizes to improve the approximation capacity of ANFIS by tuning its parameters. IPSO is used to minimize the model errors by tuning input and output MF functions through the search space provided by the ANFIS model. IPSO optimized MF functions of the developed ANFIS model while minimizing the error indices criteria.

Algorithm 1.
IPSO pseudo code (Rayen and Subhashini 2019)

```
Begin
For each and every particle
Initialize p_i and v_i of the swarm
End for
do
For each and every particle
Calculate fitness D of the particle
If D is greater than p_best
Set p_best=current fitness
End if
If p_best is better than g_best
Set g_best=best fitness value of all particles
End if
For each particle
Find v_i, update p_i
for each particle
Apply crossover and mutation
End for
End for
End for
End
```

2.2.4 Firefly algorithm (FA)

FA is designed based on the following rules that were proposed by Yang (2010): (I) all fireflies move in a more attractive and transparent way; (II) the attractive firefly is considered a brightness, which may decrease by increasing the distance from other fireflies; when there is no attractive firefly, a random move is considered; (III) the value of the objective function is used to calculate the brightness. Based on these rules, Algorithm 2 presents the processing steps of FA. Here, three components should be defined that are attractiveness, distance and movement of fireflies (Moghadam *et al*. 2019, Riahi-Madvar *et al*. 2020). The distinctive attractiveness β refers to the firefly strong attraction to other swarm members. The following equation can be used to select the attractiveness firefly

$$\beta(r) = \beta_0 e^{-\gamma(r_{ij})^m}, \qquad m \geq 1 \quad (15)$$

where, r is the distance between two fireflies, β_0 is the attractiveness at r = 0, and γ denotes a fixed light attraction coefficient.

The distance between two fireflies i and j, at positions x_i and x_j, respectively, can be calculated as follows

$$r_{ij} = \sqrt{\sum_{k=1}^{d} (x_{i,k} - x_{j,k})^2} \quad (16)$$

Algorithm 2.
FA pseudo code (Kamarian *et al*. 2014)

Objective function $f(x)$, $x = (x_1, x_2, \dots, x_d)^T$
Generate an initial population of fireflies x_i, $i = 1,2, \dots, n$
Light intensity I_i at x_i is determined by $f(x_i)$
Defined light absorption coefficient γ
While (t < Max Generation)
For i = 1:n all n fireflies
For j = 1:i all n fireflies
If ($I_j > I_i$), move firefly i towards j in d-dimensions, end if
Attractiveness varies with distance r via $\exp[-\gamma r]$
Evaluate new solutions and update light intensity
End for j
End for i
Rank the fireflies and find the current best
End while

where, $x_{i,k}$ represents the kth component of the spatial position x_i of ith firefly and d is the number of the dimensions.

The movements of a firefly (i) to another firefly (j) can be calculated as follows

$$x_i = x_i + \beta_0 e^{-\gamma(r_{ij})^2}(x_i - x_j) + \alpha\varepsilon_i \quad (17)$$

where, α and ε_i represents the randomization coefficient (between 0 and 1) and random vector, respectively.

In the current study, the FA was used to determine the optimum parameters of the MF of ANFIS for CS estimation. Here, the variations of variables should be optimized, and the fitness functions were determined. In this study, the root mean square (RMSE) is utilized as the fitness function for assessing the model performance. Each firefly comprises of a set of antecedent and subsequent parameters. For modeling, the initial population of fireflies was calculated randomly, and each firefly can be mapped to a set of ANFIS parameters. According to the light intensity related to each firefly, the attraction of each one is estimated and compared with others and fireflies with less light move toward fireflies with more light. Therefore, the RMSE value is calculated. This process continues until it reaches a determined iteration value or the least value of the target RMSE. Herein, the best solution for the FA parameters are found as follows: Light Absorption Coefficient = 2.0, Attraction Coefficient Base Value = 2, Mutation Coefficient = 0.2, and Mutation Coefficient Damping Ratio = 0.98.

2.2.5 Biogeography-based optimization (BBO)

BBO was introduced by Simon (2008). It possesses two main operations, that called migration and mutation (Ahmadlou *et al*. 2019, Jaafari *et al*. 2019). The migration is processing for sharing the features between the candidate solutions; it is used to enhance the quality of a candidate solution by modifying them using other solutions. Two migration forms are used that are emigration and immigration. Meanwhile, the mutation utilizes to improve the solution. A deep review of BBO theory can be found in (Ahmadlou *et al*. 2019, Jaafari *et al*. 2019, Simon 2008, Termeh *et al*. 2019). Here, for CS optimization, the algorithm starts with selecting a random set of residential habitats. Each habitat has k different inhabitants with its own outward and inward migration rates and specific mutation. Outward (μ_k) and inward (λ_k) migrations can be defined as the functions of the inhabitant's number in the following equations.

$$\mu_k = E\left(\frac{k}{N}\right) \quad (18)$$

$$\lambda_k = I\left(1 - \frac{k}{N}\right) \quad (19)$$

where, k represents the current inhabitants (which is calculated using the initial population based on trial-and-error method), N denotes the maximum number of eligible inhabits, and E and I are the highest rate of outward migration and inward immigration, respectively.

Another component of the optimization algorithm, mutations, can be defined as follows

$$M_k = M_{max}\left(1 - \frac{P_k}{P_{max}}\right) \quad (20)$$

where, M_k and M_{max} represent the initial and maximum mutation values, and P_k denotes the probability of mutation for the n^{th} habitat, and P_{max} is the highest value of P_k (Du *et al*. 2009).

The BBO is sensitive mainly to habitat size (N), max immigration rate for each island, migration operators and mutation probability (Simon 2008, Murlidhar *et al*. 2020). The final BBO parameters based on the trail were determined as follows: N = 30, Max immigration rate for each island = 1.0, migration operator = 1.0 and mutation probability = 0.01.

In this study, BBO was applied to calculate parameters of MF and FIS in ANFIS model; this leads to finding the best parameters of the ANFIS model for CS estimation.

2.3 Models processing and performance evaluation

The current study used five inputs (number of cycles of water magnetization (Cycles No.), age of cement mortar or paste, and cement (C), GBFS and superplasticizer (Sik) contents) to estimate the CS of cement mortar and paste.144 experimental cases were designed and used for each mortar and paste modeling. Fig. 4 presents the input and output data histograms (His) and distributions of each case. In addition, Table 3 demonstrates data distribution used in the modeling CS of cement mortar and paste. The maximum (Mx), minimum (Mn), average (Av) and skewness (Sk) of mixture cement of mortar and paste are calculated. From Fig. 4 and Table 3, it can be seen that the distribution of data for the mortar and paste is almost the same. In addition, the normal probability distribution (PD) of input and output variables imply a linear relationship between them. Moreover, the CS of cement mortar and paste has the same negative skew, and the age of both has the same positive skew. Whereas other parameters have zero skews, this means all these parameters distributions have a normal distribution around the mean value. The range of data, maximum-minimum, is approximately the same for the mixtures of cement mortar and past. These results indicate

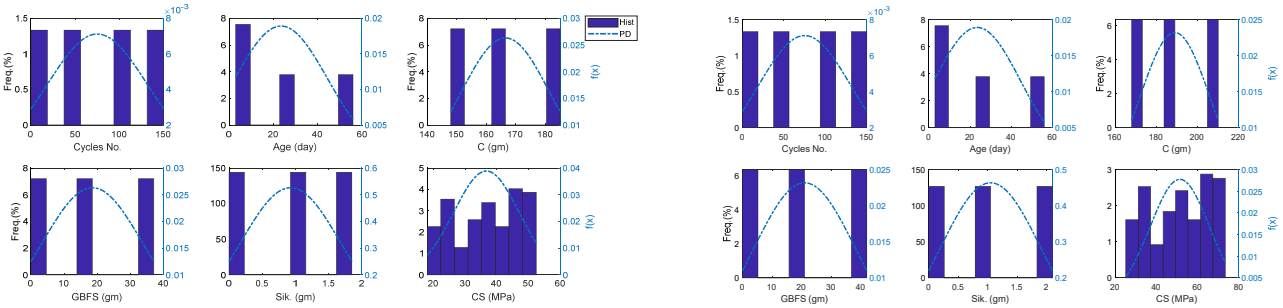

(a) (b)

Fig. 4 Histogram of inputs and output datasets along with the normal probability distribution for the (a) mortar; and (b) paste

Table 3 Statistical analysis of used data

	Cycles No.	Age (days)	C (g)	GBFS (g)	Sik. (g)	CS (MPa)
Paste						
Mx	150.00	56.00	210.00	42.00	2.10	73.44
Mn	0.00	3.00	168.00	0.00	0.00	25.20
Av	75.00	23.50	189.00	21.00	1.05	51.40
Sk	0.00	0.58	0.00	0.00	0.00	-0.23
Mortar						
Mx	150.00	56.00	185.00	37.00	1.85	52.46
Mn	0.00	3.00	148.00	0.00	0.00	18.00
Av	75.00	23.50	166.50	18.50	0.92	36.72
Sk	0.00	0.58	0.00	0.00	0.00	-0.23

that the performance of both types of mixtures is almost same for estimating the CS of mortar and paste.

Herein, for modeling the inputs and outputs variables were normalized using Eq. (21) and divided randomly into 70% (101 samples) and 30% (43 samples) for training and testing datasets of cement mortar and paste.

$$d_n = \frac{D - D_{min}}{D_{max} - D_{min}} \tag{21}$$

where, d_n represents the normalized values; D, D_{max} and D_{min} are the measured, maximum and minimum values of data used, respectively.

Fig. 2 presents the RVM model for estimating the CS, and Fig. 5 illustrates the ANFIS-FA, ANFIS-IPSO and ANFIS-BBO models.

To evaluate the performance of the proposed models, six statistical indices were used: RMSE, mean absolute error (MAE), maximum absolute error (XAE), adjusted of correlation coefficient (R^2), Pearson correlation coefficient (r) and percentage of RMSE (PE); PE indicates the percentage of model error (Kaloop *et al*. 2017).

Herein, to assess the impact of mixture contents, the sensitivity of the mixture was calculated and discussed. The impact of input variables in the optimal model was assessed. The input variable impact on the CS values of cement mortar and paste was determined using Eq. (22). A step-by-step method was carried out to obtain the sensitivity index of input variables by varying each variable at a constant rate. The sensitivity (S) of each variable can be expressed as follows (Dutta *et al*. 2018, Liong *et al*. 2000)

$$S(\%) \text{ for each variable} = \left(\frac{1}{N}\right)\sum_{j=1}^{N}\left(\frac{(\%changeinoutput)}{(\%changeininput)}\right)_j \times 100 \tag{22}$$

where, N is the number of training data points. A constant rate of 20% was selected.

3. Results and discussion

First, the performance of the proposed models (ANFIS, ANFIS-FA, ANFIS-BBO, ANFIS-IPSO and RVM) for estimating CS of cement paste is presented and evaluated. The population size is evaluated in the training stage. Table 4 presents the performance of models with changing the population size of input and output variables in mortar and paste cases. From Table 4, it can be seen that the accuracy of models is shown variable with the proposed models. This indicates that data size affects the model's accuracy. In addition, the effectiveness of population size on ANFIS-FA is shown low compared to other models. This implies that the ANFIS-FA is more stable with changing population size of available datasets. Here, to compare the proposed models

Table 4 Statistical population size effect on RMSE (MPa) of proposed models

	Sample size	RVM	ANFIS-FA	ANFIS-BBO	ANFIS-IPSO
Paste	10	3.223	1.955	4.496	4.593
	20	3.338	2.335	4.218	4.832
	50	4.556	2.353	3.742	4.432
	80	4.320	2.304	3.576	4.486
	100	4.591	2.310	3.718	4.806
Mortar	10	2.155	1.700	2.536	3.511
	20	2.469	1.892	2.088	2.794
	50	3.118	1.948	2.214	2.822
	80	2.914	1.737	2.679	3.102
	100	2.991	1.685	2.765	3.188

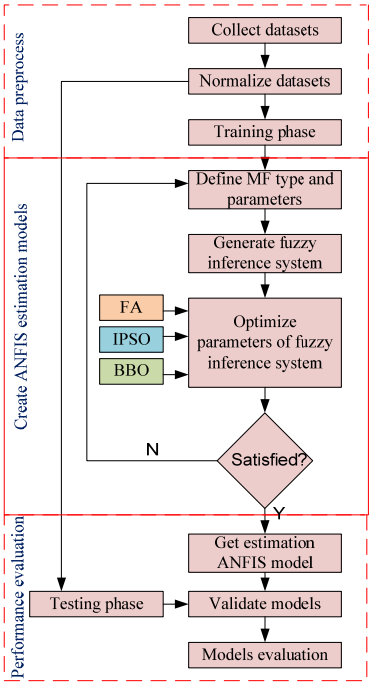

Fig. 5 ANFIS-FA, ANFIS-IPSO and ANFIS-BBO developed models for CS prediction

Table 5 Models performances for estimating CS of cement paste

	RMSE (MPa)	MAE (MPa)	XAE (MPa)	R^2 (%)	r (%)	PE (%)
Training						
RVM	4.58	4.30	9.73	87.25	93.47	9.63
ANFIS	0.00	0.00	0.00	100.00	100.00	0.00
ANFIS-FA	2.30	1.91	6.39	97.25	98.63	4.84
ANFIS-BBO	3.74	2.96	9.19	93.36	96.66	7.87
ANFIS-IPSO	4.85	4.96	13.93	82.37	90.86	10.20
Testing						
RVM	5.20	4.40	10.30	88.18	94.05	11.81
ANFIS	9.12	8.26	16.84	56.36	75.76	20.72
ANFIS-FA	2.45	2.12	6.52	96.92	98.48	5.57
ANFIS-BBO	4.39	3.65	8.99	92.19	96.11	9.96
ANFIS-IPSO	5.80	5.51	11.89	80.91	90.20	13.17

the same sample size is used in the training and testing phases.

The statistical indices of CS of cement paste for the proposed models are presented in Table 5. Figs. 6 and 7 show the performances of the proposed models in the training and testing stages, respectively. Fig. 8 shows the performance of the ANFIS model in the testing stage. The comparison of the model's performances demonstrates that the proposed ANFIS-FA model outperforms other models in training and testing stages at all statistical indices, and it is followed by the ANFIS-BBO model. In the training stage, the PE of RVM, ANFIS-FA, ANFIS-BBO and ANFIS-IPSO is 9.63%, 4.84%, 7.87% and 10.20%, respectively. And, in

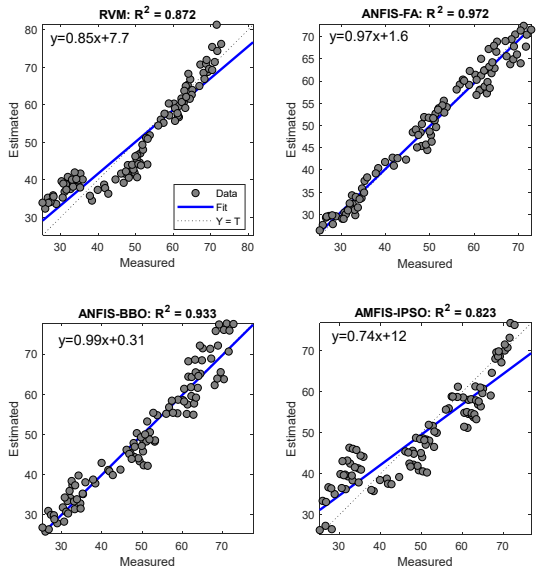

Fig. 6 Estimated to measured CS of cement paste in the training phase

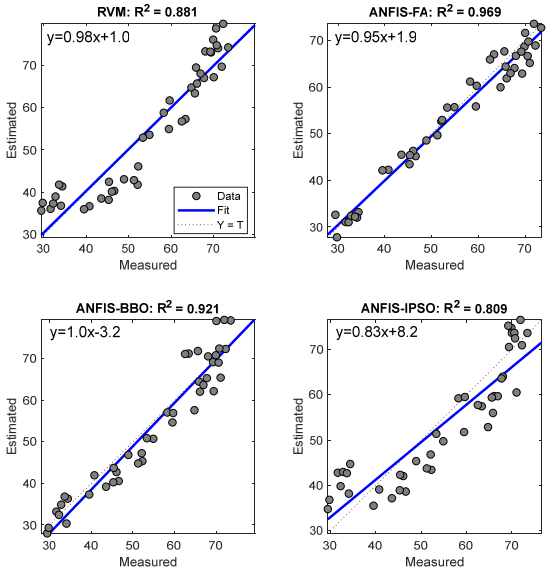

Fig. 7 Estimated to measured CS of cement paste in the testing phase

the testing stage, the PE of RVM, ANFIS-FA, ANFIS-BBO and ANFIS-IPSO is 11.81%, 5.57%, 9.96% and 13.17%, respectively. Moreover, the ANFIS performance is shown high in the training stage, while it is the worst in the testing stage. These results indicate that the accuracy of ANFIS-FA model is high and can be used to estimate the CS of cement paste with modeling error 5.20%, on average.

In addition, from Figs. 6, 7 and 8, it can be shown that the fitting line of ANFIS-FA model is highly correlated with the best fitting line in training and testing stages, R^2 = 96.92% and r = 98.48% in the testing stage. As well as, the ANFIS-BBO correlation performance is shown high with R^2 and r equal 92.19% and 96.11%, respectively. Also, a high correlation is observed with RVM model in the testing stage, r = 94.05%. But the distribution of ANFIS-FA model

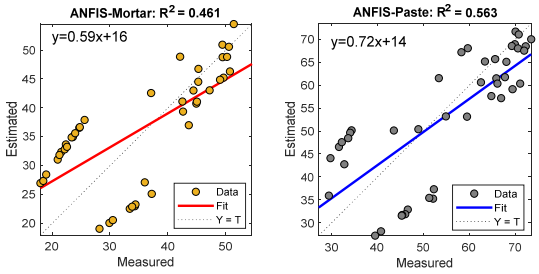

Fig. 8 Estimated to measured CS of cement paste and mortar in the testing phase

error around the best fit is shown lower than that for ANFIS-BBO and RVM models. Here, the worst models into predicting the CS of cement paste are ANFIS and ANFIS-IPSO models, respectively. From these results, it can be concluded that the ANFIS-FA model has a good performance to use as a soft computing model for estimating the CS of cement paste. Furthermore, to evaluate the model's accuracy, the regression error characteristics (REC) curved for the hybrid proposed and RVM models are assessed. Here, the absolute deviation between the measured and estimated CS of cement paste values are used to estimate the model's accuracy. Fig. 9 presents the REC curves of the hybrid proposed and RVM models for the training and testing phases. In addition, the values of the area over the curve (AOC) of REC is calculated and presented in Table 6. From Fig. 9 and Table 6, it is obviously shown that the developed ANFIS-AF model, which has low AOC values in training and testing stages, is the best model that can be used to estimate the CS of cement paste.

Secondly, the performance of the proposed models for estimating CS of cement mortar is presented and evaluated. Table 7 illustrates the statistical indices of the proposed models and Figs. 10 and 11 show the scatter plot between measured and estimated CS of cement mortar in training and testing stages, respectively. In addition, Fig. 8 presents the scatter plot of the ANFIS model for the testing stage. From Table 7 and Figs. 10 and 11, it can be seen that the performance of ANFIS-FA is also the best to estimate CS of cement mortar compared to other models. On the model error evaluation, the PE for ANFIS-FA in training and testing phases are 5.05% and 6.51%, respectively; and on the correlation between the measured and predicted CS values, the R^2 for ANFIS-FA model in training and testing stages are 96.92% and 96.20%, respectively. In addition, the distributions of ANFIS-FA model errors around the best fitting in training and testing stages are shown low compared to other models. The second model that can be used to estimate the CS of cement mortar is the developed ANFIS-BBO; all statistical indices of this model are shown lower than ANFIS-FA model and higher than RVM and ANFIS-IPSO. Moreover, the ANFIS performance is also shown high in the training stage for modeling CS of cement mortar, while it is the worst in the testing stage. Here, the worst model performance is the RVM model comparing by the hybrid ANFIS models.

From these results, it can be concluded that the ANFIS-FA model also has a good performance to use as a soft

Table 6 AOC of the proposed models for estimating CS of cement paste

Model	AOC (training)	AOC (testing)
RVM	0.088	0.089
ANFIS-FA	0.039	0.042
ANFIS-BBO	0.060	0.073
ANFIS-IPSO	0.101	0.111

Table 7 Models performances for estimating CS of cement mortar

	RMSE (MPa)	MAE (MPa)	XAE (MPa)	R^2 (%)	r (%)	PE (%)
Training						
RVM	3.00	2.69	6.33	89.07	94.44	9.00
ANFIS	0.00	0.00	0.00	100.00	100.00	0.00
ANFIS-FA	1.69	1.41	3.95	96.92	98.46	5.05
ANFIS-BBO	2.77	2.17	7.50	92.74	96.34	8.31
ANFIS-IPSO	3.20	2.78	7.51	90.04	94.94	9.58
Testing						
RVM	3.06	3.29	7.29	89.41	94.69	9.19
ANFIS	7.08	7.32	12.29	46.13	68.86	21.21
ANFIS-FA	2.17	1.70	5.24	96.20	98.13	6.51
ANFIS-BBO	3.18	2.51	7.51	92.36	96.20	9.53
ANFIS-IPSO	3.10	2.44	8.12	92.33	96.18	9.28

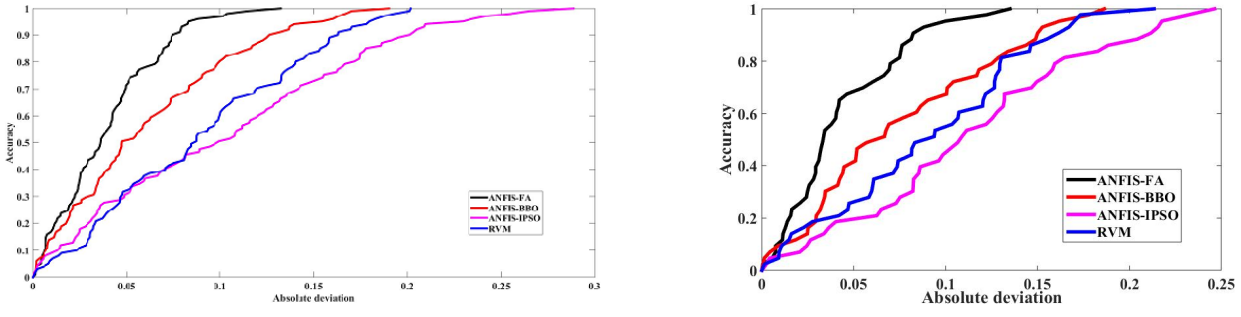

(a) (b)

Fig. 9 REC curve of the proposed models for estimating CS of cement paste in the training (a); and testing (b) phases

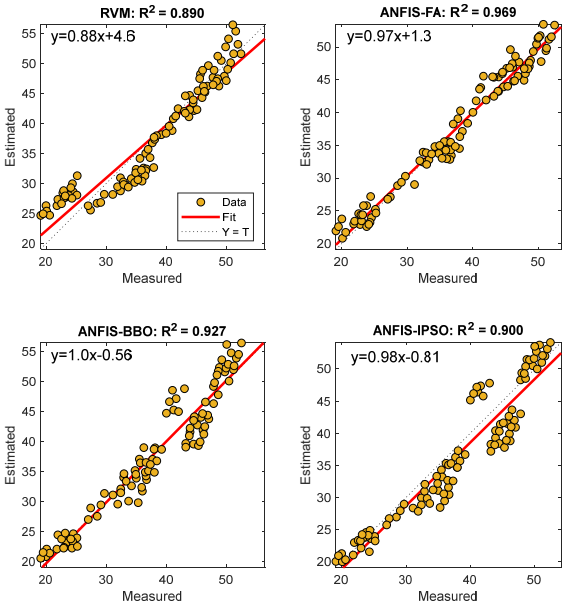

Fig. 10 Estimated to measured CS of cement mortar in the training phase

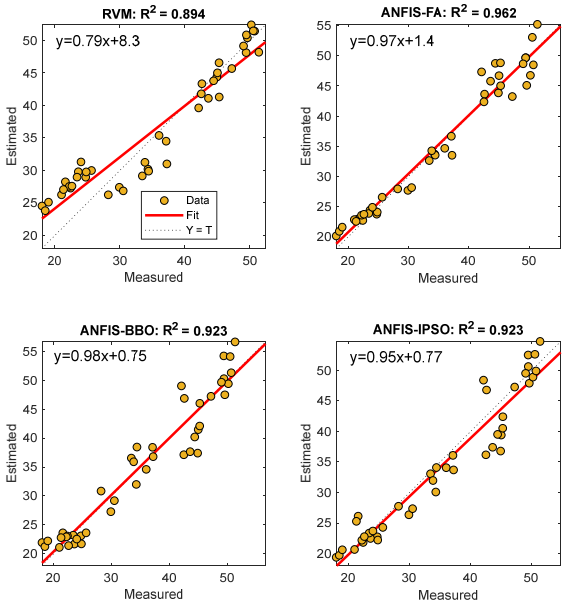

Fig. 11 Estimated to measured CS of cement mortar in the testing phase

computing model for estimating the CS of cement mortar. Also, the REC curves of the developed models for estimating CS of cement mortar are evaluated. Here, the absolute deviation between the measured and estimated CS of cement mortar values are used to estimate the model's accuracy. Fig. 12 presents the REC curves of the proposed hybrid ANFIS and RVM models for the training and testing phases. In addition, the values of AOC of REC for models of CS of cement mortar is calculated and presented in Table 8. From Fig. 12 and Table 8, it is obviously shown that the developed ANFIS-FA model, which has low AOC values in training and testing stages, is also the best model can be used to estimate the CS of cement mortar.

Here, Table 9 summarizes some of the previous studies findings and this study results in estimating the CS of

Table 8 AOC of the proposed models for estimating CS of cement mortar

Model	AOC (training)	AOC (testing)
RVM	0.077	0.093
ANFIS-FA	0.040	0.047
ANFIS-BBO	0.062	0.070
ANFIS-IPSO	0.080	0.068

Table 9 Performances ANFIS models in predicting the CS

Method	Material	R^2	Reference
ANFIS	Concrete	0.981	Gilan *et al*. (2012)
ANFIS	Mortar	0.983	Gulbandilar and Kocak (2016)
ANFIS-SC	Concrete	0.766	Mansouri *et al*. (2017)
ANFIS-FCM	Concrete	0.886	Mansouri *et al*. (2018)
ANFIS-TLBO	Mortar	0.921	Ly *et al*. (2019)
ANFIS	Concrete	0.975	Jalal *et al*. (2020)
ANFIS	Mortar	0.990	Armaghani and Asteris (2020)
ANFIS	Mortar	0.994	Madani *et al*. (2020)
ANFIS-FA	Mortar	0.962	Current study
ANFIS-FA	Paste	0.969	Current study

*ANFIS-SC: ANFIS-subtractive clustering; ANFIS-FCM: ANFIS-fuzzy c-means clustering; ANFIS-TLBO: ANFIS-Teaching-Learning-Based Optimization

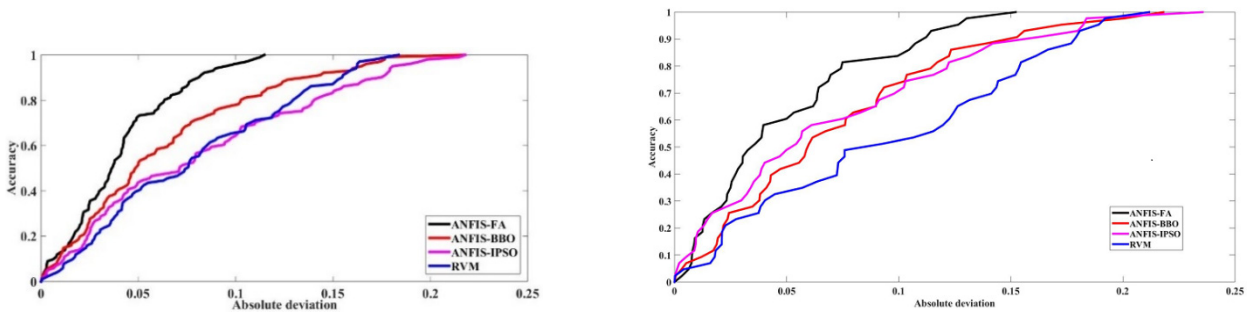

(a) (b)

Fig. 12 REC curve of the proposed models for estimating CS of cement mortar in the training (a); and testing (b) phases

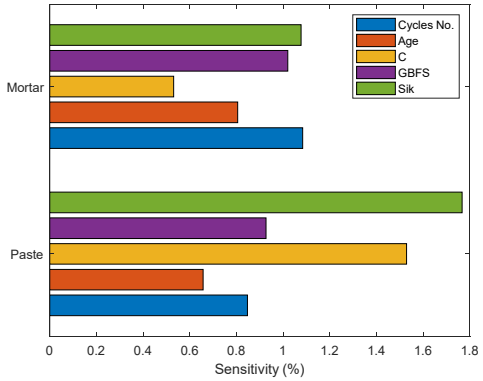

Fig. 13 Sensitivity index of input variables in ANFIS-FA model for estimating CS of paste and mortar

different concrete materials using conventional and integrated ANFIS models. From Table 9, it is clear that the ANFIS-FA model provides good performance for modeling the CS of cement mortar and paste. Furthermore, this study is new for the concrete that was prepared with MW and GBFS.

Herein, it should be mentioned that, basically, the proposed model needs the five input variables to estimate the CS of cement paste and mortar. This means the model can be applied for estimating the CS of concrete includes GBFS (0-42 g) and MW (0-150 cycles). This limits the flexibility of the proposed model for predicting the CS of the novel concrete with a huge range of GBFS and MW. In addition, although the model is a black box, it can be used as a tool to get a sense about the relationship in between the input variables for estimating the CS of concrete, as well estimate the importance of mixed contents for producing a good concrete production. Furthermore, the optimization algorithms allow identifying the unknown ANFIS black-box parameters.

Finally, the sensitivities of input variables in ANFIS-FA model for estimating CS of cement paste and mortar are calculated and presented in Fig. 13. From the figure, it can be seen that MW and GBFS both have a significant effect on the CS of cement mortar; while the cement and superplasticizer affect the CS of cement paste. Furthermore, MW affected higher than GBFS the CS of cement mortar, while via versa is shown for the CS of cement paste. The cement content and age effects are shown low for the CS of cement mortar and paste, respectively. These results indicate that the MW and GBFS have a crucial effect on the CS of cement mortar and partially affect the CS of cement paste. Whereas the superplasticizer contents were shown highly affects the CS of cement mortar and paste. This ensures the MW can replace the superplasticizer and provide similar results.

4. Conclusions

In this research, hybrid algorithms were proposed and developed. The proposed models ANFIS-FA, -IPSO and -BBO were employed and compared for estimating the CS of cement mortar and paste, which includes GBFS and prepared using MW. A total of 144 experimental sets of CS tests for each cement mortar and paste were collected. Five inputs variables were considered (i.e., cement, GBFS, cycles number of water magnetization, superplasticizer contents and curing time), and the sensitivity of them in the proposed model was evaluated in this study. The proposed models were evaluated and compared by the RVM approach, which was previously approved for predicting the CS of concrete. The developed ANFIS-FA algorithm is found to outperform other models for estimating CS of cement mortar and paste. The RMSE and R^2 of RVM, ANFIS-FA, ANFIS-BBO and ANFIS-IPO are 5.2 MPa, 2.45 MPa, 4.39 MPa, 5.80 MPa and 88.96%, 96.92%, 92.19%, 80.91%, respectively for cement paste prediction, and that for cement mortar prediction are 3.06 MPa, 2.17 MPa, 3.18 MPa, 3.10 MPa and 89.41%, 96.20%, 92.36%, 92.33%, respectively. The accuracy of ANFIS-FA model was found high compared to other models, and it can be used to estimate the CS of cement mortar and paste that include MW with modeling error 5.78% and 5.20%, in average, respectively. The sensitivities of input variables on ANFIS-FA model show that the MW and GBFS both have a significant effect on the CS of cement mortar; while the cement and superplasticizer affect the CS of cement paste. Furthermore, the MW affected higher than GBFS the CS of cement mortar, while via versa was shown for the CS of cement paste.

Acknowledgments

This work was supported by Incheon National University Research Concentration Professors Grant in 2019.

References

Aggarwal, P., Aggarwal, Y., Siddique, R., Gupta, S. and Garg, H. (2013), "Fuzzy logic modeling of compressive strength of high-strength concrete (HSC) with supplementary cementitious material", *J. Sustain. Cement-Based Mater.*, **2**(2), 128-143. https://doi.org/10.1080/21650373.2013.801800

Ahmadlou, M., Karimi, M., Alizadeh, S., Shirzadi, A., Parvinnejhad, D., Shahabi, H. and Panahi, M. (2019), "Flood susceptibility assessment using integration of adaptive network-based fuzzy inference system (ANFIS) and biogeography-based optimization (BBO) and BAT algorithms (BA)", *Geocarto Int.*, **34**(11), 1252-1272. https://doi.org/10.1080/10106049.2018.1474276

Aiyer, B.G., Kim, D., Karingattikkal, N., Samui, P. and Rao, P.R. (2014), "Prediction of compressive strength of self-compacting concrete using least square support vector machine and relevance vector machine", *KSCE J. Civil Eng.*, **18**(6), 1753-1758. https://doi.org/10.1007/s12205-014-0524-0

Akkurt, S., Tayfur, G. and Can, S. (2004), "Fuzzy logic model for the prediction of cement compressive strength", *Cement Concrete Res.*, **34**(8), 1429-1433. https://doi.org/10.1016/j.cemconres.2004.01.020

Al-Swaidani, A.M. and Khwies, W. (2018), "Applicability of Artificial Neural Networks to Predict Mechanical and Permeability Properties of Volcanic Scoria-Based Concrete", *Adv. Civil Eng.*, 2018, Article ID 5207962.

American Society for Testing and Materials International (2011),

ASTM C150- Standard Specification for Portland Cement. Annual Book of ASTM Standards. https://doi.org/10.1002/jbm.b.31853

Armaghani, D. and Asteris, P. (2020), "A comparative study of ANN and ANFIS models for the prediction of cement-based mortar materials compressive strength", *Neural Comput. Applic.* https://doi.org/10.1007/s00521-020-05244-4

ASTM Standard C33 (2003), Standard Specification for Concrete Aggregates, ASTM International. https://doi.org/10.1520/C0033

Benmouiza, K. and Cheknane, A. (2019), "Clustered ANFIS network using fuzzy c-means, subtractive clustering, and grid partitioning for hourly solar radiation forecasting", *Theor. Appl. Climatol.*, **137**, 31-43. https://doi.org/10.1007/s00704-018-2576-4

Bharath, S., Subraja, S. and Kumar, P.A. (2016), "Influence of magnetized water on concrete by replacing cement partially with copper slag", *J. Chem. Pharmaceut. Sci.*, **9**(4), 2791-2795.

Biswas, R., Samui, P. and Rai, B. (2019), "Determination of compressive strength using relevance vector machine and emotional neural network", *Asian J. Civil Eng.*, **20**(8), 1109-1118. https://doi.org/10.1007/s42107-019-00171-9

Boukhari, Y. (2020), "Using intelligent models to predict weight loss of raw materials during cement clinker production", *Revue d'Intelligence Artificielle*, **34**(1), 101-110. https://doi.org/10.18280/ria.340114

Chu, S.H. (2019), "Effect of paste volume on fresh and hardened properties of concrete", *Constr. Build. Mater.*, **218**, 284-294. https://doi.org/10.1016/j.conbuildmat.2019.05.131

Dhir, R.K., Brito, J. de, Mangabhai, R. and Lye, C.Q. (2017), "Copper Slag in Cement Manufacture and as Cementitious Material", In: *Sustainable Construction Materials*: *Copper Slag*, pp. 165-209. https://doi.org/10.1016/B978-0-08-100986-4.00005-5

Du, D., Simon, D. and Ergezer, M. (2009), "Biogeography-based optimization combined with evolutionary strategy and immigration refusal", *Proceedings of 2009 IEEE International Conference on Systems*, *Man and Cybernetics*, pp. 997-1002. https://doi.org/10.1109/ICSMC.2009.5346055

Dutta, S., Samui, P. and Kim, D. (2018), "Comparison of machine learning techniques to predict compressive strength of concrete", *Comput. Concrete*, *Int. J.*, **21**(4), 463-470. https://doi.org/10.12989/cac.2018.21.4.463

Eldessouki, M. and Hassan, M. (2015), "Adaptive neuro-fuzzy system for quantitative evaluation of woven fabrics' pilling resistance", *Expert Syst. Applic.*, **42**(4), 2098-2113. https://doi.org/10.1016/j.eswa.2014.10.013

Esfahani, A.R., Reisi, M. and Mohr, B. (2018), "Magnetized water effect on compressive strength and dosage of superplasticizers and water in self-compacting concrete", *J. Mater. Civil Eng.*, **30**(3), 1-7. https://doi.org/10.1061/(ASCE)MT.1943-5533.0002174

Gilan, S., Jovein, H. and Ramezanianpour, A. (2012), "Hybrid support vector regression – Particle swarm optimization for prediction of compressive strength and RCPT of concretes containing metakaolin", *Constr. Build. Mater.*, **34**, 321-329. https://doi.org/10.1016/j.conbuildmat.2012.02.038

Gulbandilar, E. and Kocak, Y. (2016), "Application of expert systems in prediction of flexural strength of cement mortars", *Comput. Concrete*, *Int. J.*, **18**(1), 1-16. https://doi.org/10.12989/cac.2016.18.1.001

Hesami, M., Naderi, R., Tohidfar, M. and Yoosefzadeh-Najafabadi, M. (2019), "Application of Adaptive Neuro-Fuzzy Inference System-Non-dominated Sorting Genetic Algorithm-II (ANFIS-NSGAII) for Modeling and Optimizing Somatic Embryogenesis of Chrysanthemum", *Frontiers Plant Sci.*, **10**, 869. https://doi.org/10.3389/fpls.2019.00869

Jaafari, A., Panahi, M., Pham, B.T., Shahabi, H., Bui, D.T., Rezaie, F. and Lee, S. (2019), "Meta optimization of an adaptive neuro-fuzzy inference system with grey wolf optimizer and biogeography-based optimization algorithms for spatial prediction of landslide susceptibility", *Catena*, **175**, 430-445. https://doi.org/10.1016/j.catena.2018.12.033

Jalal, M., Grasley, Z., Gurganus, C. and Bullard, J.W. (2020), "Experimental investigation and comparative machine-learning prediction of strength behavior of optimized recycled rubber concrete", *Constr. Build. Mater.*, **256**, 119478. https://doi.org/10.1016/j.conbuildmat.2020.119478

Kaloop, M.R., El-diasty, M., Hu, J.W. and El-diasty, M. (2017), "Real-time prediction of water level change using adaptive neuro-fuzzy inference system", *Geomat. Natural Hazard. Risk*, **8**(2), 1320-1332. https://doi.org/10.1080/19475705.2017.1327464

Kamarian, S., Yas, M.H., Pourasghar, A. and Daghagh, M. (2014), "Application of firefly algorithm and ANFIS for optimisation of functionally graded beams", *J. Experim. Theor. Artif. Intell.*, **26**, 197-209. https://doi.org/10.1080/0952813X.2013.813978

Khorshidi, N., Ansari, M. and Bayat, M. (2014), "An investigation of water magnetization and its influence on some concrete specificities like fluidity and compressive strength", *Comput. Concrete*, *Int. J.*, **13**(5), 649-657. https://doi.org/10.12989/cac.2014.13.5.649

Kockal, N. (2015), "Optimizing production parameters of ceramic tiles incorporating fly ash using response surface methodology", *Ceramics Int.*, **41**, 14529-14536. https://doi.org/10.1016/j.ceramint.2015.07.168

Kockal, N., Beycan, O. and Gulmez, N. (2017), "Physical and mechanical properties of silica fume and calcium hydroxide based geopolymers", *Acta Physica Polonica A*, **131**(3), 530-533. https://doi.org/10.12693/APhysPolA.131.530

Kockal, N., Beycan, O. and Gulmez, N. (2018), "Effect of binder type and content on physical and mechanical properties of geopolymers", *Sadhana*, **43**, Article No. 49. https://doi.org/10.1007/s12046-018-0806-1

Liong, S.-Y., Lim, W.-H. and Paudyal, G. (2000), "River stage forecasting in Bangladish: Neural network approach", *J. Comput. Civil Eng.*, **14**(1), 1-8. https://doi.org/10.1061/(ASCE)0887-3801(2000)14:1(1)

Ly, H.B., Pham, B.T., Dao, D.V., Le, V.M., Le, L.M. and Le, T.T. (2019), "Improvement of ANFIS model for prediction of compressive strength of manufactured sand concrete", *Appl. Sci.*, **9**(18), 3841. https://doi.org/10.3390/app9183841

Ma, B., Mei, J., Tan, H., Li, H., Liu, X., Jiang, W. and Zhang, T. (2019), "Effect of Nano Silica on Hydration and Microstructure Characteristics of Cement High Volume Fly Ash System Under Steam Curing", *J. Wuhan Univ. Technol.-Mater. Sci. Ed.*, **34**(3), 604-613. https://doi.org/10.1007/s11595-019-2094-y

Madani, H., Kooshafar, M. and Emadi, M. (2020), "Compressive Strength Prediction of Nanosilica-Incorporated Cement Mixtures Using Adaptive Neuro-Fuzzy Inference System and Artificial Neural Network Models", *Pract. Period. Struct. Des. Constr.*, **25**(3), 04020021. https://doi.org/10.1061/(ASCE)SC.1943-5576.0000499

Mansouri, I., Ozbakkaloglu, T., Kisi, O. and Xie, T. (2016), "Predicting behavior of FRP-confined concrete using neuro fuzzy, neural network, multivariate adaptive regression splines and M5 model tree techniques", *Mater. Struct./Materiaux et Constr.*, **49**(10), 4319-4334. https://doi.org/10.1617/s11527-015-0790-4

Mansouri, I., Kisi, O., Sadeghian, P., Lee, C.H. and Hu, J.W. (2017), "Prediction of ultimate strain and strength of FRP-confined concrete cylinders using soft computing methods", *Appl. Sci.*, **7**(8), 751. https://doi.org/10.3390/app7080751

Mansouri, I., Gholampour, A., Kisi, O. and Ozbakkaloglu, T.

(2018), "Evaluation of peak and residual conditions of actively confined concrete using neuro-fuzzy and neural computing techniques", *Neural Comput. Applic.*, **29**(3), 873-888. https://doi.org/10.1007/s00521-016-2492-4

Mansouri, I., Shariati, M., Safa, M., Ibrahim, Z., Tahir, M.M. and Petković, D. (2019), "Analysis of influential factors for predicting the shear strength of a V-shaped angle shear connector in composite beams using an adaptive neuro-fuzzy technique", *J. Intell. Manuf.*, **30**(3), 1247-1257.

Mishra, M., Bhatia, A.S. and Maity, D. (2019a), "A comparative study of regression, neural network and neuro-fuzzy inference system for determining the compressive strength of brick–mortar masonry by fusing nondestructive testing data", *Eng. Comput.*, **37**, 77-91. https://doi.org/10.1007/s00366-019-00810-4

Mishra, M., Bhatia, A.S. and Maity, D. (2019b), "Support vector machine for determining the compressive strength of brick-mortar masonry using NDT data fusion (case study: Kharagpur, India)", *SN Appl. Sci.*, **1**(6), 564. https://doi.org/10.1007/s42452-019-0590-5

Moghadam, R.G., Izadbakhsh, M.A., Yosefvand, F. and Shabanlou, S. (2019), "Optimization of ANFIS network using firefly algorithm for simulating discharge coefficient of side orifices", *Appl. Water Sci.*, **9**(4), 1-12. https://doi.org/10.1007/s13201-019-0950-8

Murthy, A.R., Vishnuvardhan, S., Saravanan, M. and Gandhi, P. (2019), "Relevance vector based approach for the prediction of stress intensity factor for the pipe with circumferential crack under cyclic loading", *Struct. Eng. Mech., Int. J.*, **72**(1), 31-41. https://doi.org/10.12989/sem.2019.72.1.793

Murlidhar, B.R., Kumar, D., Armaghani, D.J., Mohamad, E.T., Roy, B. and Pham, B.T. (2020), "A novel intelligent ELM-BBO technique for predicting distance of mine blasting-induced flyrock", *Natural Resour. Res.*, **29**, 4103-4120. https://doi.org/10.1007/s11053-020-09676-6

Pannu, H.S., Singh, D. and Malhi, A.K. (2018), "Improved particle swarm optimization based adaptive neuro-fuzzy inference system for benzene detection", *CLEAN - Soil, Air, Water*, **46**(5), 1700162. https://doi.org/10.1002/clen.201700162

Prasad Meesaraganda, L.V., Sarkar, N. and Tarafder, N. (2020), "Adaptive Neuro-Fuzzy Inference System for Predicting Strength of High-Performance Concrete", In: *Advances in Intelligent Systems and Computing*, Springer, Singapore pp. 119-134. https://doi.org/10.1007/978-981-15-0035-0_10

Prasanna, P.K., Ramachandra Murthy, A. and Srinivasu, K. (2018), "Prediction of compressive strength of GGBS based concrete using RVM", *Struct. Eng. Mech., Int. J.*, **68**(6), 691-700. https://doi.org/10.12989/sem.2018.68.6.691

Qadir, W., Ghafor, K. and Mohammed, A. (2019), "Evaluation the effect of lime on the plastic and hardened properties of cement mortar and quantified using Vipulanandan model", *Open Eng.*, **9**(1), 468-480. https://doi.org/10.1515/eng-2019-0055

Rahchamani, G., Movahedifar, S.M. and Honarbakhsh, A. (2019), "A hybrid optimized learning-based compressive performance of concrete prediction using GBMO-ANFIS classifier and genetic algorithm reduction", *Struct. Concrete*, suco.201900155. https://doi.org/10.1002/suco.201900155

Rayen, S.J. and Subhashini, R. (2019), "Mammogram image retrieval using IPSO optimized anfis classifier", *Int. J. Innov. Technol. Explor. Eng.*, **8**(9 Special Issue 2), 799-804. https://doi.org/10.35940/ijitee.I1165.0789S219

Razavi Tosee, S.V. and Nikoo, M. (2019), "Neuro-fuzzy systems in determining light weight concrete strength", *J. Central South Univ.*, **26**(10), 2906-2914. https://doi.org/10.1007/s11771-019-4223-3

Riahi-Madvar, H., Dehghani, M., Parmar, K.S., Nabipour, N. and Shamshirband, S. (2020), "Improvements in the explicit estimation of pollutant dispersion coefficient in rivers by subset selection of maximum dissimilarity hybridized with ANFIS-firefly algorithm (FFA)", *IEEE Access*, **8**, 60314-60337. https://doi.org/10.1109/ACCESS.2020.2979927

Safiuddin, M., Raman, S., Abdus Salam, M. and Jumaat, M. (2016), "Modeling of compressive strength for self-consolidating high-strength concrete incorporating palm oil fuel ash", *Materials*, **9**(5), 396. https://doi.org/10.3390/ma9050396

Selma, B., Chouraqui, S. and Abouaïssa, H. (2020), "Optimal trajectory tracking control of unmanned aerial vehicle using ANFIS-IPSO system", *Int. J. Inform. Technol.*, **12**(2), 383-395. https://doi.org/10.1007/s41870-020-00436-6

Seo, J. and Pokhrel, J. (2019), "Surrogate modeling for self-consolidating concrete characteristics estimation for efficient prestressed bridge construction", *ACI Special Publication*, **333**, pp. 19-39.

Seo, J., Kim, Y. and Zandyavari, S. (2015), "Response Surface Metamodel-based Performance Reliability for Reinforced Concrete Beams Strengthened with FRP sheets", *ACI Special Publication*, **304**, pp. 1-20.

Seo, J., Torres, E. and Schaffer, W. (2017), "Self-Consolidating Concrete for Prestressed Bridge Girders", Report; South Dakota State University, USA.

Simon, D. (2008), "Biogeography-based optimization", *IEEE Transact. Evolution Computat.*, **12**(6), 702-713. https://doi.org/10.1109/TEVC.2008.919004

Sinha, D.K., Rupali, S. and Bawa, S. (2019), "Application of Adaptive Neuro- Fuzzy Inference System for the prediction of Early Age Strength of High Performance Concrete", *Proceedings of 2019 International Conference on Data Science and Engineering* (*ICDSE*), 1-5. https://doi.org/10.1109/ICDSE47409.2019.8971798

Su, N., Wu, Y.-H. and Mar, C.-Y. (2000), "Effect of magnetic water on the engineering properties of concrete containing granulated blast-furnace slag", *Cement Concrete Res.*, **30**(4), 599-605. https://doi.org/10.1016/S0008-8846(00)00215-5

Tayfur, G., Erdem, T.K. and Kırca, Ö. (2014), "Strength Prediction of High-Strength Concrete by Fuzzy Logic and Artificial Neural Networks", *J. Mater. Civil Eng.*, **26**(11), 04014079. https://doi.org/10.1061/(ASCE)MT.1943-5533.0000985

Taylor, P., Yurdakul, E., Ceylan, H. and Bektas, F. (2012), "Effect of Paste Quality on Fresh and Hardened Properties of Ternary Mixtures", In: *IOWA State University* (Vol. DTFH61-06-). https://doi.org/10.1016/j.conbuildmat.2019.05.131

Termeh, S.V.R., Khosravi, K., Sartaj, M., Keesstra, S.D., Tsai, F. T.C., Dijksma, R. and Pham, B.T. (2019), "Optimization of an adaptive neuro-fuzzy inference system for groundwater potential mapping", *Hydrogeol. J.*, **27**(7), 2511-2534. https://doi.org/10.1007/s10040-019-02017-9

Tipping, M.E. (2000), "Sparse Bayesian learning and the relevance vector machine", *J. Mach. Learn. Res.*, **1**, 211-244. https://doi.org/10.1162/15324430152748236

Torres, E. and Seo, J. (2017), "State-of-the-art and practice review and recommended testing protocol: self-consolidating concrete for prestressed bridge girders", *Eur. J. Environ. Civil Eng.*, **21**(12), 1419-1440. https://doi.org/10.1080/19648189.2016.1170730

Torres, E., Seo, J. and Lederle, R. (2017), "Experimental and Statistical Investigation of Self-Consolidating Concrete Mixture Constituents for Prestressed Bridge Girder Fabrication", *J. Mater. Civil Eng.*, **29**(9), 04017141. https://doi.org/10.1061/(ASCE)MT.1943-5533.0001968

Verma, M., Thirumalaiselvi, A. and Rajasankar, J. (2017), "Kernel-based models for prediction of cement compressive strength", *Neural Comput. Applic.*, **28**(S1), 1083-1100. https://doi.org/10.1007/s00521-016-2419-0

Wang, Y., Wei, H. and Li, Z. (2018), "Effect of magnetic field on

the physical properties of water", *Results in Phys*., **8**, 262-267. https://doi.org/10.1016/j.rinp.2017.12.022

Xiao, Y., Liu, J.J., Hu, Y., Wang, Y., Lai, K.K. and Wang, S. (2014), "A neuro-fuzzy combination model based on singular spectrum analysis for air transport demand forecasting", *J. Air Transport Manage*., **39**, 1-11. https://doi.org/10.1016/j.jairtraman.2014.03.004

Yang, X.S. (2010), "Firefly algorithm, stochastic test functions and design optimization", *Int. J. Bio-Inspired Computat*., **2**(2), 78. https://doi.org/10.1504/IJBIC.2010.032124

Yousry, O.M.M., Abdallah, M.A., Ghazy, M.F., Taman, M.H. and Kaloop, M.R. (2020), "A Study for Improving Compressive Strength of Cementitious Mortar Utilizing Magnetic Water", *Materials*, **13**, 1971. https://doi.org/10.3390/ma13081971

Yuvaraj, P., Murthy, A.R., Iyer, N.R., Samui, P. and Sekar, S. (2014), "Prediction of fracture characteristics of high strength and ultra high strength concrete beams based on relevance vector machine", *Int. J. Damage Mech*., **23**(7), 979-1004. https://doi.org/10.1177/1056789514520796

CC

Appendix A

Table A1 Mixture proportions of mortar mixes (% of binders) incorporating (W/B = 0.4). (B = CEM + GBFS)

Mix ID	CEM (I) (%)	GBFS (%)	SP (%)	No. of cycles	Sand (%)	Mix ID	CEM (I) (%)	GBFS (%)	Sik (%)	No. of cycles	Sand (%)
TM-000-0.0-00	**100**	**0**	**0**	**0**	**300**	**MM-050-0.0-00**	**100**	**0**	**0**	**50**	**300**
TM-000-0.0-10	**90**	**10**	**0**	**0**	**300**	**MM-050-0.0-10**	**90**	**10**	**0**	**50**	**300**
TM-000-0.0-20	**80**	**20**	**0**	**0**	**300**	**MM-050-0.0-20**	**80**	**20**	**0**	**50**	**300**
TM-000-0.5-00	**100**	**0**	**0.5**	**0**	**300**	**MM-050-0.5-00**	**100**	**0**	**0.5**	**50**	**300**
TM-000-0.5-10	**90**	**10**	**0.5**	**0**	**300**	**MM-050-0.5-10**	**90**	**10**	**0.5**	**50**	**300**
TM-000-0.5-20	**80**	**20**	**0.5**	**0**	**300**	**MM-050-0.5-20**	**80**	**20**	**0.5**	**50**	**300**
TM-000-1.0-00	**100**	**0**	**1**	**0**	**300**	**MM-050-1.0-00**	**100**	**0**	**1**	**50**	**300**
TM-000-1.0-10	**90**	**10**	**1**	**0**	**300**	**MM-050-1.0-10**	**90**	**10**	**1**	**50**	**300**
TM-000-1.0-20	**80**	**20**	**1**	**0**	**300**	**MM-050-1.0-20**	**80**	**20**	**1**	**50**	**300**
MM-100-0.0-00	**100**	**0**	**0**	**100**	**300**	**MM-150-0.0-00**	**100**	**0**	**0**	**150**	**300**
MM-100-0.0-10	**90**	**10**	**0**	**100**	**300**	**MM-150-0.0-10**	**90**	**10**	**0**	**150**	**300**
MM-100-0.0-20	**80**	**20**	**0**	**100**	**300**	**MM-150-0.0-20**	**80**	**20**	**0**	**150**	**300**
MM-100-0.5-00	**100**	**0**	**0.5**	**100**	**300**	**MM-150-0.5-00**	**100**	**0**	**0.5**	**150**	**300**
MM-100-0.5-10	**90**	**10**	**0.5**	**100**	**300**	**MM-150-0.5-10**	**90**	**10**	**0.5**	**150**	**300**
MM-100-0.5-20	**80**	**20**	**0.5**	**100**	**300**	**MM-150-0.5-20**	**80**	**20**	**0.5**	**150**	**300**

Table A2 Mixture proportions of paste mixes (% of binders) incorporating (W/B = 0.28)

Mix ID	CEM (I) (%)	GBFS (%)	SP (%)	No. of cycles	Mix ID	CEM (I) (%)	GBFS (%)	Sik (%)	No. of cycles
TP-000-0.0-00	**100**	**0**	**0**	**0**	**MP-050-0.0-00**	**100**	**0**	**0**	**50**
TP-000-0.0-10	**90**	**10**	**0**	**0**	**MP-050-0.0-10**	**90**	**10**	**0**	**50**
TP-000-0.0-20	**80**	**20**	**0**	**0**	**MP-050-0.0-20**	**80**	**20**	**0**	**50**
TP-000-0.5-00	**100**	**0**	**0.5**	**0**	**MP-050-0.5-00**	**100**	**0**	**0.5**	**50**
TP-000-0.5-10	**90**	**10**	**0.5**	**0**	**MP-050-0.5-10**	**90**	**10**	**0.5**	**50**
TP-000-0.5-20	**80**	**20**	**0.5**	**0**	**MP-050-0.5-20**	**80**	**20**	**0.5**	**50**
TP-000-1.0-00	**100**	**0**	**1**	**0**	**MP-050-1.0-00**	**100**	**0**	**1**	**50**
TP-000-1.0-10	**90**	**10**	**1**	**0**	**MP-050-1.0-10**	**90**	**10**	**1**	**50**
TP-000-1.0-20	**80**	**20**	**1**	**0**	**MP-050-1.0-20**	**80**	**20**	**1**	**50**
MP-100-0.0-00	**100**	**0**	**0**	**100**	**MP-150-0.0-00**	**100**	**0**	**0**	**150**
MP-100-0.0-10	**90**	**10**	**0**	**100**	**MP-150-0.0-10**	**90**	**10**	**0**	**150**
MP-100-0.0-20	**80**	**20**	**0**	**100**	**MP-150-0.0-20**	**80**	**20**	**0**	**150**
MP-100-0.5-00	**100**	**0**	**0.5**	**100**	**MP-150-0.5-00**	**100**	**0**	**0.5**	**150**
MP-100-0.5-10	**90**	**10**	**0.5**	**100**	**MP-150-0.5-10**	**90**	**10**	**0.5**	**150**
MP-100-0.5-20	**80**	**20**	**0.5**	**100**	**MP-150-0.5-20**	**80**	**20**	**0.5**	**150**
MP-100-0.5-00	**100**	**0**	**0.5**	**100**	**MP-150-0.5-00**	**100**	**0**	**0.5**	**150**
MP-100-0.5-10	**90**	**10**	**0.5**	**100**	**MP-150-0.5-10**	**90**	**10**	**0.5**	**150**
MP-100-0.5-20	**80**	**20**	**0.5**	**100**	**MP-150-0.5-20**	**80**	**20**	**0.5**	**150**